

## **Formation of plutonium (IV) silicate species in very alkaline reactive media**

Estevenon, P.; Dumas, T.; Lorenzo Solari, P.; Welcomme, E.; Szenknect, S.; Mesbah, A.; Kvashnina, K. O.; Moisy, P.; Poinssot, C.; Dacheux, N.;

Originally published:

July 2021

**Dalton Transactions 50(2021), 12528-12536**

DOI: <https://doi.org/10.1039/D1DT02248B>

Perma-Link to Publication Repository of HZDR:

<https://www.hzdr.de/publications/Publ-32876>

Release of the secondary publication  
on the basis of the German Copyright Law § 38 Section 4.

# Formation of plutonium (IV) silicate species in very alkaline reactive media

Paul Estevenon<sup>1,2,3,4</sup>, Thomas Dumas<sup>1,\*</sup>, Pier Lorenzo Solari<sup>5</sup>, Eleonore Welcomme<sup>1</sup>,  
Stephanie Szenknect<sup>2</sup>, Adel Mesbah<sup>2</sup>, Kristina O. Kvashnina<sup>3,4</sup>, Philippe Moisy<sup>1</sup>, Christophe  
Poinssot<sup>1</sup>, Nicolas Dacheux<sup>2,\*</sup>

<sup>1</sup> CEA, DES, ISEC, DMRC, Univ Montpellier, Marcoule, France.

<sup>2</sup> ICSM, Univ Montpellier, CNRS, CEA, ENSCM, Bagnols-sur-Cèze, France

<sup>3</sup> The Rossendorf Beamline at the European Synchrotron, CS40220, 38000 Grenoble Cedex 9, France.

<sup>4</sup> Helmholtz Zentrum Dresden-Rossendorf (HZDR), Institute of Resource Ecology, P.O. Box 510119, 01314, Dresden, Germany.

<sup>5</sup> Synchrotron SOLEIL L'Orme des Merisiers, Saint-Aubin, BP 48, F-91192 Gif-sur-Yvette Cedex France

## ABSTRACT:

The formation of stable plutonium (IV) silicate colloidal suspension has been identified in very alkaline reactive media ( $\text{pH} \geq 13$ ). XAS measurements allowed to observe that these species exhibit a structure similar to those reported at (IV) oxidation state, like for thorium, uranium and neptunium silicates counterparts. These colloids can be stabilized in aqueous solution at concentrations around  $10^{-2} \text{ mol}\cdot\text{L}^{-1}$  and successive filtration process allowed to evaluate that most of these silicates had a size ranging between 3 and 6 nm. This result may bring new outlooks on the behavior of plutonium in silicate ions rich reactive media.

Keywords: plutonium (IV), plutonium (IV) silicate, actinide (IV) silicate colloids, EXAFS measurements

## 1. INTRODUCTION

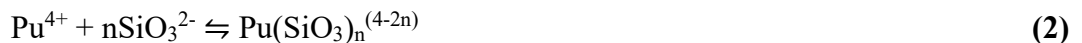
Actinides, and mainly plutonium, are the main contributors to the long-term radiotoxicity of spent nuclear fuel.<sup>1</sup> In conditions representative of a geological repository, the interactions between such radioelements and silicate species could influence the mobility of the actinides in the environment<sup>2-4</sup> and thus, could affect the safety of the storage facilities.

Even if the formation of plutonium silicate complexes has been reported, plutonium (IV) chemistry in silicate environment remains poorly understood. Among them,  $\text{Pu}(\text{OSi}(\text{OH})_3)^{3+}$  was prepared between pH 0.3 and 1.4 in diluted aqueous plutonium and silicate solution and a  $\log(\beta^\circ) = 11.8$  (1) value was evaluated according to equation (1).<sup>5</sup>



Pazukhin *et al.*<sup>6</sup> observed that the titration of Pu(IV) in nitric solution by a aqueous sodium metasilicate solution did not lead to the precipitation of plutonium hydroxide up to pH = 12 while its precipitation occurred at pH = 2 – 4 for a titration performed with NaOH or  $\text{NH}_4\text{OH}$  without metasilicate. They attributed these results to the formation of a plutonium silicate complex with a  $[\text{Pu}(\text{IV})]:[\text{Na}_2\text{SiO}_3] = 1:8$  mole ratio.<sup>6</sup> However, these results and especially the pH values reported should be considered with caution. Indeed, the Pu(IV) hydrolysis and the precipitation of plutonium hydroxide generally occurs below pH = 1 in non-complexing reactive media.<sup>7</sup> Moreover, the UV-visible spectra obtained are very similar to those reported by Yusov *et al.* for  $\text{Pu}(\text{OSi}(\text{OH})_3)^{3+}$ .<sup>5</sup>

Shilov and Fedoseev<sup>8</sup> also observed that silicate species have an impact on the Pu(IV) solubility in alkaline conditions, pH = 11 – 13.8, leading to plutonium concentrations around  $10^{-8} \text{ mol}\cdot\text{L}^{-1}$ ,<sup>8</sup> after ultrafiltration with 10 kDa filters (i.e. pores diameter 2.8 nm),<sup>9</sup> against  $4 \times 10^{-11} \text{ mol}\cdot\text{L}^{-1}$  in silicate free reactive media.<sup>7</sup> This increase of solubility was attributed to the potential formation of  $\text{Pu}^{\text{IV}}(\text{SiO}_3)_n^{(4-2n)}$  species following reaction (2). However, Shilov and Fedoseev didn't observe any impact of silicate ions on plutonium solubility at pH = 9, unlike the results reported by Pazukhin *et al.*<sup>6</sup>



Experiments performed with thorium(IV) and neptunium(IV) in silicate reactive media also led to the formation of  $\text{An}(\text{OSi}(\text{OH})_3)^{3+}$  complexes.<sup>5, 10</sup> Moreover, silicate ions have been identified to have a strong impact on thorium solubility in alkaline reactive media due to the formation of a thorium hydroxo-silicate complex,  $[\text{Th}(\text{OH})_3(\text{OSi}(\text{OH})_3)_3]^{2-}$ , which has been evidenced in these conditions.<sup>11</sup>

Furthermore, the formation of actinide silicate colloids has been reported for thorium(IV),<sup>2, 12-15</sup> uranium(IV)<sup>3, 14-17</sup> and neptunium(IV)<sup>4, 15, 18</sup> (**Table 1**). The stability and mobility of these actinide bearing silicate colloids under environmental conditions strongly differed from the oxy-hydroxide colloids due to their low isoelectric point ( $\text{pH}_{\text{IEP}}(\text{Th}) = 4.6$ ,<sup>2</sup>  $\text{pH}_{\text{IEP}}(\text{U}) = 4.4$ <sup>3</sup> and  $\text{pH}_{\text{IEP}}(\text{Np}) = 2.6$ <sup>4, 18</sup> against  $\text{pH}_{\text{IEP}}$  close to 8 for the respective actinide oxy-hydroxides colloids<sup>18</sup>). These colloids correspond to 1 – 20 nm particles at low silicate ions concentrations (below silicic acid mononuclear wall;  $[\text{Si}] = 2 \times 10^{-3} \text{ mol}\cdot\text{L}^{-1}$ <sup>19</sup>) and ~ 200 nm agglomerates at higher concentrations. Moreover, structural characterizations performed by EXAFS spectroscopy<sup>2-4, 14-16, 18</sup> allowed to observe that the actinide coordination shell in these silicate colloids was analogous to the one determined for solid actinide (IV) silicates,  $\text{AnSiO}_4$ , (zircon type structure).<sup>20</sup> However, even if the formation of actinide silicate colloids has clearly been identified in carbonate ions rich reactive media, the formation of these species in carbonate ions free reactive media has only been suspected for thorium in alkaline conditions and may also be suspected for plutonium (**Table 1**).<sup>2-4, 8, 11, 13, 16-18</sup>

**Table 1** Conditions reported for the formation of actinide (IV) silicate colloids in carbonate ions rich reactive media and in carbonate ions free reactive media, where their formation was suspected (after ultrafiltration of the corresponding solutions).

<b>Observation in carbonate ions rich reactive media</b>					
<b>Reference</b>	<b>Actinide-silicate system</b>	<b>Conditions</b>	<b>pH</b>	<b>Colloids size</b>	
				<b>Below MWSA</b>	<b>Above MWSA</b>
[2]	Th-silicate	$[\text{NaHCO}_3] = 0.05 \text{ mol}\cdot\text{L}^{-1}$ $[\text{Th}] = 10^{-3} \text{ mol}\cdot\text{L}^{-1}$ $\text{Si/Th} = 0.3 - 8$	$\geq 7$	7 – 20 nm	
[3, 16]	U-silicate	$[\text{NaHCO}_3] = 0.05 \text{ mol}\cdot\text{L}^{-1}$ $[\text{U}] = 10^{-3} \text{ mol}\cdot\text{L}^{-1}$ $\text{Si/U} = 0.25 - 3$	7 – 9.5	$\leq 20$ nm	
[17]	U-silicate	$[\text{NaHCO}_3] = 0.05 \text{ mol}\cdot\text{L}^{-1}$ $[\text{U}] = 10^{-3} \text{ mol}\cdot\text{L}^{-1}$ $\text{Si/U} = 2 - 4$	9 – 10.5	1 – 10 nm	$\leq 220$ nm
[4, 18]	Np-silicate	$[\text{NaHCO}_3] = 0.1 \text{ mol}\cdot\text{L}^{-1}$ $[\text{Np}] = 10^{-3} \text{ mol}\cdot\text{L}^{-1}$ $\text{Si/Np} = 0.7 - 8.6$	7 – 9	5 nm	$\leq 250$ nm
<b>Observation in carbonate ions free reactive media</b>					
<b>Reference</b>	<b>Actinide-silicate system</b>	<b>Conditions</b>	<b>pH</b>	<b>remarks</b>	
[13]	Th-silicate	$\text{ThO}_2 \cdot x\text{H}_2\text{O}$ $[\text{Si}] = 10^{-3} - 0.15 \text{ mol}\cdot\text{L}^{-1}$	6 – 12	ThO <sub>2</sub> solubility increase	
[11]	Th-silicate	$\text{ThO}_2 \cdot x\text{H}_2\text{O}$ $[\text{Si}] = 1.8 \times 10^{-2} \text{ mol}\cdot\text{L}^{-1}$	10 – 13.3	ThO <sub>2</sub> solubility increase	
[8]	Pu-silicate	$\text{PuO}_2 \cdot x\text{H}_2\text{O}$ $[\text{Si}] = 10^{-3} - 10^{-2} \text{ mol}\cdot\text{L}^{-1}$	11 – 13.8	PuO <sub>2</sub> solubility increase	

*MWSA : Mononuclear wall of silicic acid*

In this work, the experiments were focused on the chemistry of Pu(IV) in very alkaline silicate ions reactive media, in order to provide an explanation on the solubility increase of PuO<sub>2</sub> reported in the literature. However, unlike the previous literature's experiments, we chose to work in nearly saturated silicate ions reactive media, in order to facilitate the identification of the potential Pu(IV)-silicate species obtained in these conditions.

## 2. MATERIALS AND METHODS

### 2.1. Samples preparation

*Caution!*  $^{238}\text{Pu}$ ,  $^{239}\text{Pu}$ ,  $^{240}\text{Pu}$  and  $^{242}\text{Pu}$  are  $\alpha$ -emitter and  $^{241}\text{Pu}$  is  $\beta$ -emitter which are considered as a health risk. Experiments involving actinides require appropriate facilities and trained persons in handling of radioactive materials.

Experiments were performed at the ATALANTE Facility of Marcoule Research Centre, France. The stock solution of plutonium (isotope mixture: 0.04%  $^{238}\text{Pu}$ , 95.77%  $^{239}\text{Pu}$ , 3.70%  $^{240}\text{Pu}$ , 0.14%  $^{241}\text{Pu}$ , 0.35%  $^{242}\text{Pu}$ ) was purified by a standard anion-exchange method, in order to remove  $^{241}\text{Am}$  produced by  $\beta$ -decay of  $^{241}\text{Pu}$  product.<sup>21</sup> Plutonium was stabilized in the oxidation state +IV, in a  $1.5 \text{ mol}\cdot\text{L}^{-1}$   $\text{HNO}_3$  solution. It was then titrated by UV-visible spectroscopic method, by standard deconvolution from reference measurements ( $C_{\text{Pu}} = 0.30 \pm 0.03 \text{ mol}\cdot\text{L}^{-1}$ ).

An aqueous silicate solution was prepared by dissolving  $\text{Na}_2\text{SiO}_3\cdot 9\text{H}_2\text{O}$  (98%) supplied by Sigma-Aldrich in water in order to obtain a nearly saturated aqueous solution ( $C_{\text{Na}_2\text{SiO}_3} \approx 2 \text{ mol}\cdot\text{L}^{-1}$ ). Experiments were performed by adding of the Pu(IV) stock solution to 0.8 mL of the silicate solution under vigorous stirring (500 rpm). Then, the pH of the reactive media was controlled. The precipitates obtained were separated from the supernatant by centrifugation for 14 min at 14,000 rpm, corresponding to a cut-off of size around 150 nm according to the calculation method described by Livshits *et al.*<sup>22</sup>. UV-visible and XAS measurements were performed on the as-obtained supernatant.

In order to evaluate the size of the colloids, additional experiments were performed from the raw aqueous solutions which were centrifugated 10 min à 4,500 rpm (corresponding to a cut-off of size around  $550 \text{ nm}$ )<sup>22</sup>, in order to eliminate the largest precipitated particles. The solution was then filtrated thanks to Whatman® Anotop  $0.45 \mu\text{m}$ ,  $0.1 \mu\text{m}$  and  $0.02 \mu\text{m}$  syringe filters and ultrafiltrated thanks Merck® Amicon Ultra to 100 kDa, 10 kDa and 3 kDa filters units (i.e. pores diameters 6.1 nm, 2.9 nm and 2.0 nm, respectively)<sup>9</sup>. Aliquots were taken at each filtration step in order to measure the concentration of plutonium thanks to  $\alpha$  counting measurements and to perform additional characterizations.

### 2.1. Characterization

All of the UV-visible spectrometric measurements were performed on a Varian Cary 6000i spectrometer installed outside of the cell with a fiber-optic signal transmission line.

Measurements were performed in quartz cells between  $\lambda = 350$  nm and 900 nm. Due to the specific analysis conditions with long glass fibers between the spectrometer and the sample located in a glovebox, it was not possible to use the molar coefficients of plutonium in nitric acid media reported in the literature. Therefore, deconvolutions of the spectra were performed using reference spectra of actinide solutions with known concentrations previously recorded in the same conditions.

The Extended X-ray Absorption Fine Structure (EXAFS) and X-Ray Absorption Near Edge Structure (XANES) spectroscopy measurements were carried out at the MARS beamline at the SOLEIL synchrotron facility (Saint-Aubin).<sup>23</sup> The spectra were collected in the fluorescence mode with a 13 element Ge detector at ambient temperature. Measurements have been performed at the plutonium L<sub>III</sub> edge (18057 eV). Data reduction and extraction of EXAFS oscillation was performed using the Athena and Artemis package.<sup>24</sup> The threshold energy,  $E_0$ , was defined as the maximum of the first derivative of the absorption coefficient. Experimental EXAFS spectra were Fourier Transformed (FT) using a Hanning window over the k-space range 2–11 Å<sup>-1</sup>. The shell fits were performed in R-space on the k<sup>3</sup> weighted FT EXAFS oscillations. Theoretical phase shifts and backscattering amplitudes were obtained with the ab initio code FEFF8.2<sup>25</sup> using the reference PuSiO<sub>4</sub> and CeSiO<sub>4</sub> structures.<sup>26,27</sup>

The concentration of Pu in colloidal solutions was determined by  $\alpha$  – spectrometry (7401 Canberra) performed at the energy of <sup>239</sup>Pu  $\alpha$  – decay. The spectrometer was calibrated with sealed sources samples with known activities. Prior the measurement, the samples were diluted and a determined volume was deposited on a stainless steel sample holder and then evaporated by heating.

pH determinations were performed with a Metrohm pH electrode, allowing pH measurement on the 0-14 pH range, calibrated thanks to pH = 2.00, 7.00 and 12.45 buffer solutions.

### 3. RESULTS AND DISCUSSION

Preparation of a nearly saturated  $\text{Na}_2\text{SiO}_3$  solution led to the very alkaline aqueous reactive media ( $\text{pH} \approx 13.3$ ). Adding a Pu(IV) nitric acid solution to this  $\text{Na}_2\text{SiO}_3$  solution led to a pH decrease (Table S1 and Figure S1) and allowed to observe the formation of aqueous plutonium species for  $\text{pH} \geq 13$  (Figure 1), characterized by the absorption bands observed at  $\lambda = 455, 486, 526, 551, 584, 633, 654, 677, 755$  and  $793$  nm. The as-obtained alkaline plutonium silicates were green-colored solutions and remained stable for months (Figure S2). Decreasing the pH of the reactive media led to gelation for  $\text{pH} \leq 13$  and a strong decrease of the plutonium solubility. Measurements performed at  $\text{pH} \leq 12$  did not allow the identification of aqueous plutonium species. This behavior could be explained by silicate ions protonation, considering  $\text{HSiO}_3^-/\text{SiO}_3^{2-}$  or  $\text{H}_3\text{SiO}_4^-/\text{H}_2\text{SiO}_4^{2-}$  acid dissociation constants. The associated constant values were evaluated to  $\text{pK}_A = 11.99$ <sup>28</sup> and  $\text{pK}_A = 13.30$ <sup>29</sup>, respectively. This would drastically change the chemical conditions in the reactive media, modify the silicate species solubility and thus the gelation conditions in the reactive media. Moreover, it might be inferred that protonated silicate based species (e.g.  $\text{H}_3\text{SiO}_4^-$ ) would present a lower affinity regarding to plutonium compared to  $\text{SiO}_3^{2-} / \text{H}_2\text{SiO}_4^{2-}$  ions.

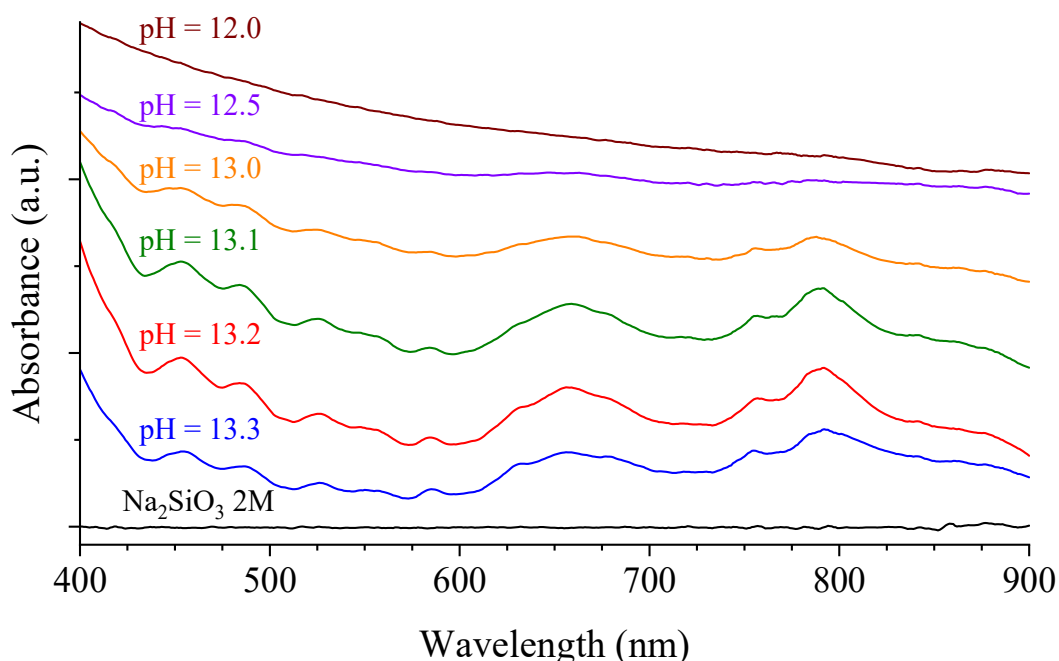


**Figure 1** UV-visible spectra of Pu(IV) in a  $2 \text{ mol}\cdot\text{L}^{-1}$   $\text{Na}_2\text{SiO}_3$  solution depending on the pH of the reactive media (i.e. amount of Pu(IV) in  $\text{HNO}_3$   $1 \text{ mol}\cdot\text{L}^{-1}$  added)

The comparison with aqueous plutonium oxo-hydroxo colloids solution allowed to observe that the as-obtained plutonium species did not correspond to hydrolyzed plutonium (**Figure 2**) nor to the plutonium silicate complex,  $\text{PuOSi(OH)}_3^{3+}$ , reported by Pazukhin *et al.*<sup>6</sup> and Yusov *et al.*<sup>5</sup> but might correspond to aqueous plutonium silicate species, such as  $\text{Pu(SiO}_3)_n^{(4-2n)}$  proposed by Shilov and Fedoseev<sup>8</sup> however, to the best of our knowledge, no UV-visible spectra of that specie was reported. Putting an aliquot of alkaline plutonium silicate in  $1 \text{ mol}\cdot\text{L}^{-1} \text{ HNO}_3$  led to the full dissociation of the silicate species, evidenced by the obtention of UV-vis spectra characteristic of Pu(IV) in 1 M nitric acid. The solution was characterized a few minutes after the acidification and no change of the corresponding UV-vis spectra was observed over time, corresponding to a fast dissociation process, corresponding to a very different behavior from that of the nearly insoluble plutonium oxo-hydroxy colloids. This protocol allowed to determine the Pu concentration in solution using UV-vis spectroscopy. In the Pu silicate solution at  $\text{pH} = 13.2$ , the highest Pu concentration measured was  $C_{\text{Pu}} = 3 \times 10^{-2} \text{ mol}\cdot\text{L}^{-1}$ , however, the colloids formation seems to be very sensitive to the experimental conditions and most of the measurement on these solutions led to concentration around  $10^{-2} \text{ mol}\cdot\text{L}^{-1}$  (Figure S1)

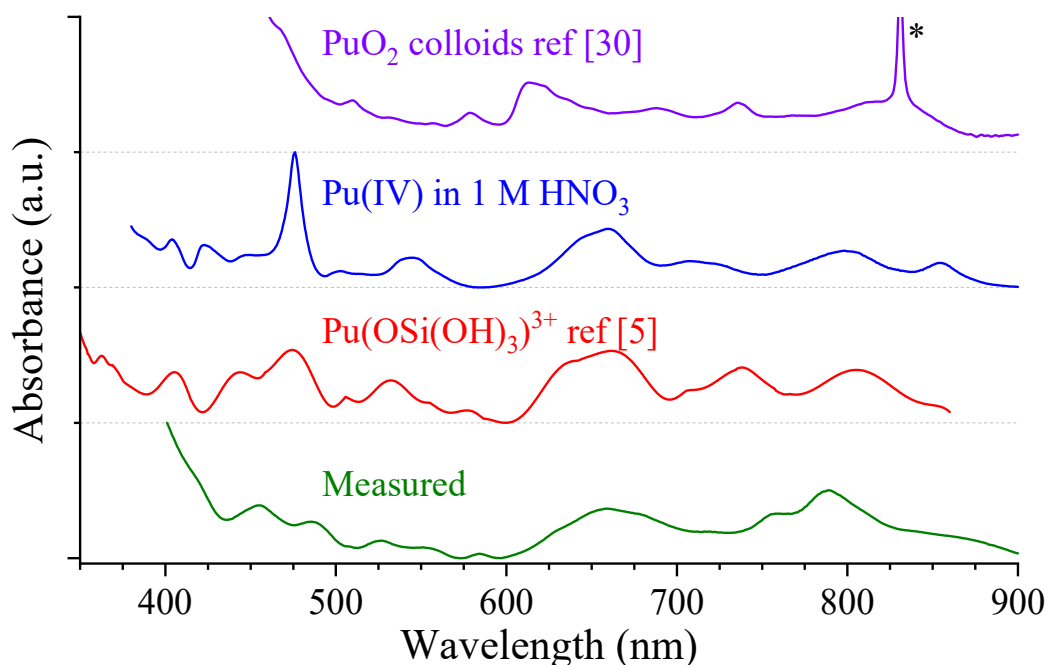


**Figure 2** UV-visible spectrum of a Pu(IV)-silicate solution ( $\text{pH} = 13.2$ ,  $C_{\text{Na}_2\text{SiO}_3} \approx 2 \text{ mol}\cdot\text{L}^{-1}$ ,  $C_{\text{Pu}} = 3 \times 10^{-2} \text{ mol}\cdot\text{L}^{-1}$ ), compared with the spectra reported by Dalodière *et al.*<sup>30</sup> for Pu(IV) colloidal solution ( $\text{PuO}_2^{2+}$  observed as impurities at  $\lambda = 830 \text{ nm}$ , identified by an asterisk), with that of the  $\text{Pu(OSi(OH)}_3)^{3+}$  complex reported by Yusov *et al.*<sup>5</sup> and that of a Pu(IV) solution prepared in  $1 \text{ mol}\cdot\text{L}^{-1} \text{ HNO}_3$ .

Filtration experiments have been performed on the plutonium silicate colloidal solution to check if the obtained species corresponding to complexes or colloidal particles. A sequential filtration process was performed on the raw solution centrifuged during 10 min at 4,500 rpm (cut off of size around 550 nm)<sup>22</sup> then filtered at 0.45  $\mu\text{m}$ , 0.1  $\mu\text{m}$ , 0.02  $\mu\text{m}$ , 100 kDa (6.1 nm)<sup>9</sup>, 10 kDa (2.9 nm)<sup>9</sup> and 3 kDa (2.0 nm)<sup>9</sup>. The plutonium concentration after filtration was measured by  $\alpha$  spectrometry (**Figure 3a** and **Table 2**). It was measured around  $(12 \pm 2) \times 10^{-3} \text{ mol}\cdot\text{L}^{-1}$  for the sample filtered at 0.45  $\mu\text{m}$  and decreased down to  $(8.4 \pm 0.8) \times 10^{-3} \text{ mol}\cdot\text{L}^{-1}$  to reach a plateau for filtration steps at 0.1  $\mu\text{m}$ , 0.02  $\mu\text{m}$ , 100 kDa. This first decrease could be assigned to the elimination of the largest particles present in solution. It allowed discriminating the size of the plutonium silicate species measured to be below 6.1 nm<sup>9</sup>. It is worth noting that the particle agglomeration, which has been generally described for actinide silicate colloids formed above the silicic acid mononuclear wall,<sup>4, 17, 18</sup> was not observed in that case. It might be explained by the very alkaline conditions considered leading to nanoparticles with negative surface charge which could have minimized the agglomeration tendency due to electrostatic repulsion. The concentration obtained for the filtration at 10 kDa and 3 kDa were measured to  $(2.7 \pm 0.3) \times 10^{-3} \text{ mol}\cdot\text{L}^{-1}$  and  $(1.7 \pm 0.3) \times 10^{-3} \text{ mol}\cdot\text{L}^{-1}$ . These results demonstrated that the particles observed were in the colloidal state with a quite homogeneous size distribution and a median size ranging from 6.1 nm to 2.9 nm.<sup>9</sup> This size is consistent with that obtained for PuO<sub>2</sub> nanoparticles (i.e. 2 to 3 nm).<sup>30-34</sup> The plutonium concentration after filtrations at 10 kDa and 3 kDa remained quite high for such alkaline plutonium aqueous solutions. This result might be explained by different hypotheses: the presence of very small Pu-silicate colloidal particles, solution leaks or membrane breaks of the filter units which could have allowed the partial diffusion of plutonium species or the formation of Pu-silicate complexes. This last hypothesis might be compared to the formation of  $[\text{Th}(\text{OH})_3(\text{OSi}(\text{OH})_3)_3]^{2-}$  complexes which has been suggested in literature for thorium in silicate rich and alkaline media.<sup>11</sup> However, it was not clearly evidenced for plutonium in this study.

Additionally, UV-vis spectra were measured on the filtered solution aiming at verifying the nature of the species obtained (**Figure 3b**). For the filtration above 100 kDa, the spectra have been found to be similar to the ones previously reported (**Figure 1** and **Figure 2**). The statement on the elimination of the largest suspended nanoparticles, between the filtration steps at 0.45  $\mu\text{m}$  and 0.1  $\mu\text{m}$ , was confirmed by UV-vis spectroscopy, with the decrease of the background absorbance at  $\lambda < 600 \text{ nm}$  which could be attributed to Mie scattering. According

to the results expected by Beer Lambert law, nearly no additional difference was observed between the supernatants obtained after filtration at 0.1  $\mu\text{m}$ , 0.02  $\mu\text{m}$  and 100 kDa. Indeed, the only slight modification observed could be due to the elimination of  $\text{SiO}_2$  colloids. However, one other strong decrease in intensity was observed when performing the filtration at 10 kDa or at 3 kDa. All of these results are in good agreement with a particle size distribution with a median size ranging from 6.1 nm to 2.9 nm.

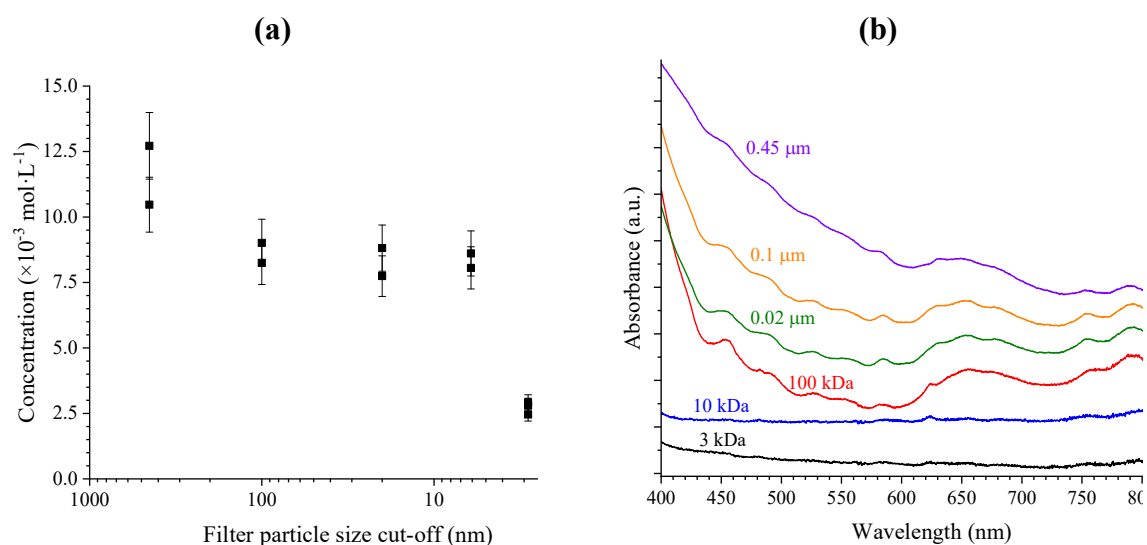


**Figure 3** Pu(IV)-silicate solution ( $\text{pH} = 13.2$ ,  $C_{\text{Na}_2\text{SiO}_3} \approx 2 \text{ mol}\cdot\text{L}^{-1}$ ) concentration determined by alpha spectroscopy (a) and UV-visible spectra (b) for solutions filtrated at 0.45  $\mu\text{m}$ , 0.1  $\mu\text{m}$ , 0.02  $\mu\text{m}$ , 100 kDa, 10 kDa and 3 kDa.

**Table 2** Pu(IV)-silicate solution ( $\text{pH} = 13.2$ ,  $C_{\text{Na}_2\text{SiO}_3} \approx 2 \text{ mol}\cdot\text{L}^{-1}$ ) concentration determined by alpha spectrometry for solutions filtrated at 0.45  $\mu\text{m}$ , 0.1  $\mu\text{m}$ , 0.02  $\mu\text{m}$ , 100 kDa, 10 kDa and 3 kDa.

Filter cut-off	Measured concentrations ( $\times 10^{-3} \text{ mol}\cdot\text{L}^{-1}$ )*		
0.45 $\mu\text{m}$	10.4	12.7	
0.1 $\mu\text{m}$	8.25	9.01	
0.02 $\mu\text{m}$	7.74	8.81	
100 kDa (6.1 nm)	8.61	8.06	
10 kDa (2.9 nm)	2.92	2.80	2.46
3 kDa (2.0 nm)	1.76	1.69	1.68

\* Measurement uncertainty: 10%

In order to determine the structure of these plutonium silicate colloids, XAS measurements were performed at plutonium  $L_{III}$  edge. First, the XANES spectrum carried out on this sample enabled the identification of Pu(IV) as the predominant oxidation state, from its characteristic maximum absorption peak at 18068 eV and because of the absence of the shoulder feature at 18082 eV typical of Pu(V) or Pu(VI) (**Figure 4**), confirming the tetravalent oxidation state of plutonium in the considered silicate species.

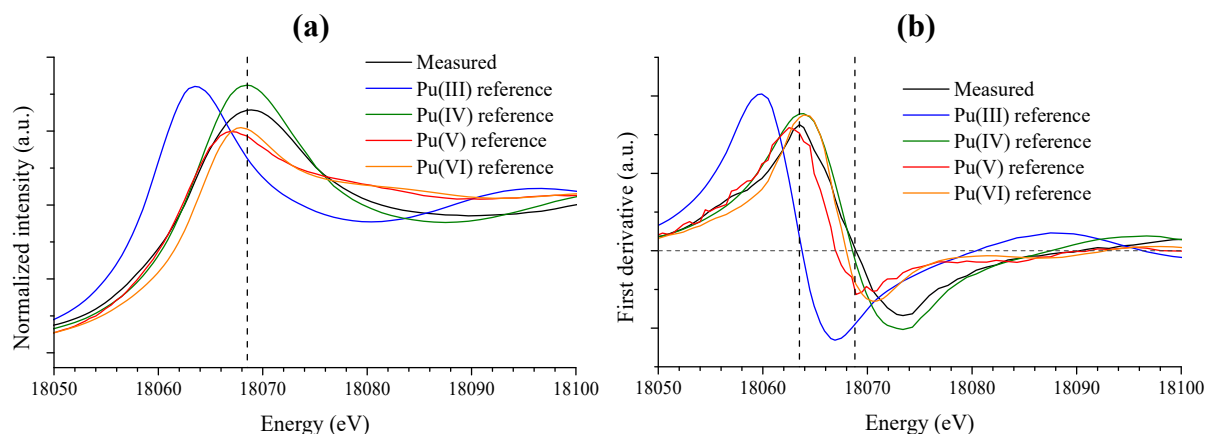


**Figure 4** XANES spectra (a) and respective first derivative (b) at plutonium  $L_{III}$  edge for a Pu(IV)-silicate solution with  $C_{Na_2SiO_3} = 2 \text{ mol}\cdot\text{L}^{-1}$ ,  $C_{Pu} \approx 10^{-2} \text{ mol}\cdot\text{L}^{-1}$  and  $\text{pH} = 13.2$ .

Secondarily, the plutonium coordination sphere was studied using the pseudo-radial distribution function obtained from the Fourier Transform of the EXAFS oscillations (**Figure 5**). From the EXAFS spectrum and corresponding FT, it was already possible to exclude the formation of intrinsic plutonium oxy-hydroxide colloids by comparison with previously reported EXAFS spectra.<sup>30, 35, 36</sup> The obtained spectra exhibited similarities with the actinide silicate colloids already identified for thorium(IV), uranium(IV) and neptunium(IV).<sup>2-4, 17</sup> For these three actinide silicate systems, three main scattering shells were distinguished on the Fourier Transform: a first peak at  $R + \Delta = 1.6 \text{ \AA}$  attributed to the An(IV)-Oxygen interactions, the second shell at  $2.3 \text{ \AA} \leq R + \Delta \leq 3.2 \text{ \AA}$  attributed to A(IV)-Si interactions and for  $3.0 \text{ \AA} \leq R + \Delta \leq 4.0 \text{ \AA}$ , An(IV)-An(IV) interactions were evidenced. This suggests structural similarities between these colloids and the aqueous plutonium silicate species obtained in this work. Therefore, the model used for the analysis of the EXAFS measurement was based on the data treatment performed for each of these actinide silicate colloids. Consequently, the structure was derived from those reported in the literature for tetravalent

actinide silicates, AnSiO<sub>4</sub> (**Table S2**). Because PuSiO<sub>4</sub> and CeSiO<sub>4</sub> are reported to be isostructural<sup>26, 27</sup> and octacoordinated, Pu<sup>4+</sup> and Ce<sup>4+</sup> exhibit close ionic radii ( $r(\text{VIII Pu}^{4+}) = 0.96 \text{ \AA}$  ;  $r(\text{VIII Ce}^{4+}) = 0.97 \text{ \AA}$ ),<sup>37</sup> the atomic positions of oxygen, which are not reported in the PuSiO<sub>4</sub> structure, were considered to be similar to those reported for CeSiO<sub>4</sub>. In the model used for the fit of the EXAFS spectra, coordination numbers, interatomic distances and Debye-Waller factors were taken as adjustment variables. However, since the structure of the measured species is very disordered and too much free parameters did not allowed the model to merge to reasonable values, the number of oxygen atoms were fixed and the Debye Waller parameters for Pu-Si were chosen to be in the same range as the value reported in the literature for the An-silicate colloids (**Table S3**).

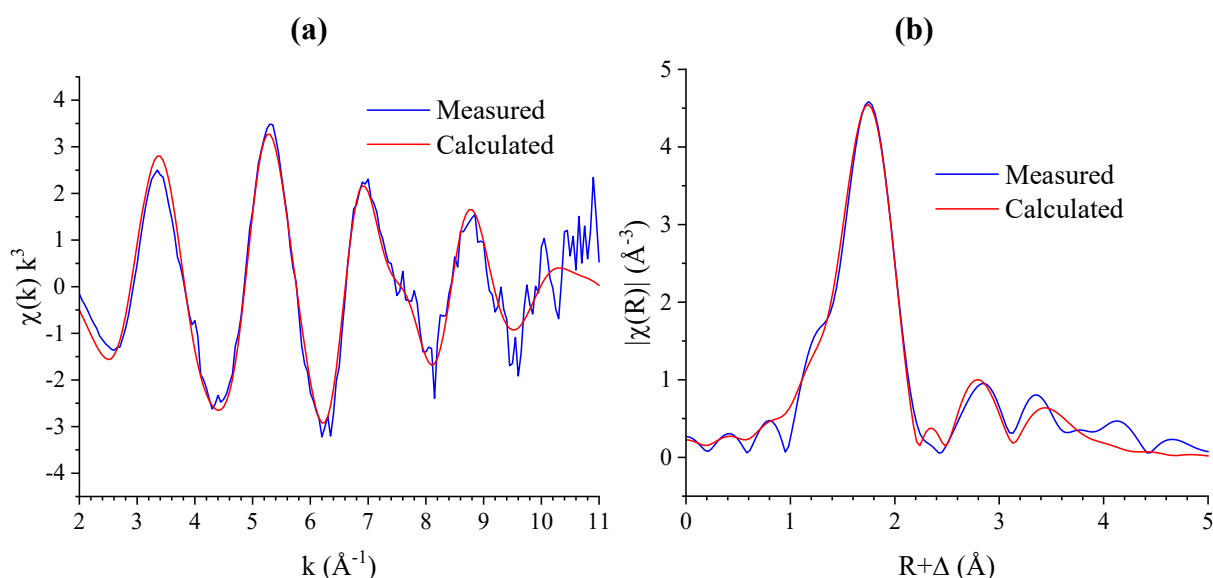


**Figure 5** EXAFS spectra  $2 \text{ \AA} < k < 11 \text{ \AA}^{-1}$  (a) and respective Fourier Transform (b) at plutonium L<sub>III</sub> edge for a Pu(IV)-silicate solution with  $C_{\text{Na}_2\text{SiO}_3} = 2 \text{ mol}\cdot\text{L}^{-1}$ ,  $C_{\text{Pu}} \approx 10^{-2} \text{ mol}\cdot\text{L}^{-1}$  and  $\text{pH} = 13.2$ .

The first peak and its shoulder obtained for the pseudo-radial distribution function were hence attributed to oxygen atoms in the first coordination sphere of plutonium,  $R(\text{Pu-O}_1) = 2.23(2) \text{ \AA}$  and  $R(\text{Pu-O}_2) = 2.34(3) \text{ \AA}$  (**Figure 5** and **Table 3**) in good agreement with the values reported in the literature for  $R(\text{An-O})$  (i.e.  $2.2 - 2.5 \text{ \AA}$ ) (**Table S3**). The two next peaks have been attributed to silicon atoms in the second coordination sphere of plutonium and correspond to the presence of bidentate and monodentate silicate groups. Consistently with previous hypotheses from Hennig *et al.*<sup>2</sup>, Neill *et al.*<sup>17</sup> and Husar *et al.*<sup>4</sup>, bidentate silicate groups correspond to shorter Pu-Si distances ( $R(\text{Pu-Si}_1) = 3.21(6) \text{ \AA}$ ) than monodentate groups

( $R(\text{Pu-Si}_2) = 3.46(3) \text{ \AA}$ ). The resulting coordination numbers for silicates show more monodentate groups and less bidentate groups than that was expected ( $\text{CN}(\text{Pu-Si}_2) = 5.4(22)$  and  $\text{CN}(\text{Pu-Si}_1) = 1.1(9)$  against  $\text{CN}(\text{Pu-Si}_2) = 4$  and  $\text{CN}(\text{Pu-Si}_1) = 2$ ) and might indicate a disordered structure. At further distance, a third contribution may be assigned to the plutonium-plutonium interactions. The quite low intensity of this contribution,  $\text{CN}(\text{Pu-Pu}) = 6.0(21)$ , and the high Debye Waller parameter associated ( $\sigma^2(\text{Pu-Pu}) = 0.020(26) \text{ \AA}^2$ ) indicate that the long-range structure is disordered. All of these results, on both the interatomic distance measured and the structural disorder, are consistent with the results already reported for An(IV)-silicate colloids, with An = Th, U and Np (**Table 4**). Moreover, considering the distances reported for the solid  $\text{CeSiO}_4$  and  $\text{USiO}_4$  and extrapolated for  $\text{PuSiO}_4$ , the Pu-Si and Pu-Pu distances are in good agreement with the formation of a tetravalent plutonium silicate compound (**Table 3**). These observations support the previous hypothesis of the formation of amorphous An(IV) silicate particles in which the local structure of plutonium is a disordered An(IV) silicate-like structure.

**Table 3** Structural parameters determined for Pu(IV)-silicate species ( $C_{\text{Na}_2\text{SiO}_3} = 2 \text{ mol}\cdot\text{L}^{-1}$ ,  $C_{\text{Pu}} \approx 10^{-2} \text{ mol}\cdot\text{L}^{-1}$  and  $\text{pH} = 13.2$ ) and expected interatomic distances for  $\text{PuSiO}_4$ .<sup>26</sup> The values fixed for the simulations have been marked by an asterisk.  $\Delta E_{k=0} = -1.4 \text{ eV}$ ,  $F = 0.07$ ,  $S_0^2 = 0.9$ .

	R (Å)	N	$\sigma^2$ (Å <sup>2</sup> )	Expected R (Å) for $\text{PuSiO}_4$
Pu-O <sub>1</sub>	2.23 (2)	4 *	0.007 (3)	---
Pu-O <sub>2</sub>	2.34 (3)	4 *	0.007 (3)	---
Pu-Si <sub>1</sub>	3.21 (6)	1.1 (9)	0.009*	3.11
Pu-Si <sub>2</sub>	3.46 (3)	5.4 (22)	0.012*	3.79
Pu-Pu	3.77 (3)	6.0 (21)	0.020 (26)	3.79

**Table 4** Structural parameters determined for Pu(IV)-silicate species ( $C_{\text{Na}_2\text{SiO}_3} = 2 \text{ mol}\cdot\text{L}^{-1}$ ,  $C_{\text{Pu}} \approx 10^{-2} \text{ mol}\cdot\text{L}^{-1}$  and  $\text{pH} = 13.2$ ) and reported in the literature for An(IV)-silicate colloids. Uncertainties were omitted for clarity; all of the data are available in Table S3.

An	Th <sup>2</sup>	U <sup>16</sup>	U <sup>17</sup>	Np <sup>2</sup>	Pu (this study)
An-O <sub>1</sub>	R = 2.36–2.39 Å N = 8.3–8.9	R = 2.23–2.25 Å N = 2.7–4.1	R = 2.23–2.30 Å N = 3.7–4.7	R = 2.28 Å N = 7.1	R = 2.23 Å N = 4
An-O <sub>2</sub>			R = 2.44–2.47 Å N = 3.0–3.9		R = 2.34 Å N = 4
An-Si <sub>1</sub>	R = 3.23–3.26 Å N = 1.3–2.5	R = 2.81–2.83 Å N = 2.7–3.5	R = 3.17–3.19 Å N = 0.9–1.6	R = 3.11 Å N = 1.3	R = 3.21 Å N = 1.1
An-Si <sub>2</sub>			R = 3.70–3.76 Å N = 0.8–2.5		R = 3.46 Å N = 5.4
An-An	---	R = 3.85 Å N = 2.6	R = 3.78–3.86 Å N = 1.0–5.0	R = 3.75 Å N = 1.1	R = 3.77 Å N = 6.0

Therefore, the plutonium species obtained in silicate ions rich and very alkaline reactive media may be attributed to the formation of plutonium silicate-based colloids close to those reported for the other actinide silicate colloids (**Table S3**) with a short-distance environment similar to the one expected for PuSiO<sub>4</sub>. The small size of the colloidal particles, range from 2.9 to 6.1 nm for Pu-Pu distances measured at 0.377 nm, might also explain the strong disorder observed in EXAFS, because of the over-representation of the plutonium located on the surface of the nanoparticles compared to the ones located in the core of the colloids (roughly representing 30-60% of the Pu atoms for that size of nanoparticles).

Moreover, in order to describe the nature of the samples and to rule out any important change on aged and filtered samples, EXAFS spectra have been recorded on the solutions filtered at 0.45 μm and 100 kDa and the one-year aged system filtered at 100 kDa prior the ageing. The  $k^3$  weighted spectra and corresponding Fourier Transforms as well as the best fit parameters are presented in **Figure 6** and **Table S3**. Overall, the EXAFS signal does not exhibit noticeable differences considering uncertainties and the plutonium silicate colloids structure is unaltered. Indeed, the main Pu-O contributions, as well as second sphere Pu-Si and Pu-Pu contributions, are still present. Consequently, the plutonium species observed could clearly be identified as plutonium (IV) bearing silicate colloids and it has been evidenced that these colloidal suspensions were stable over time.

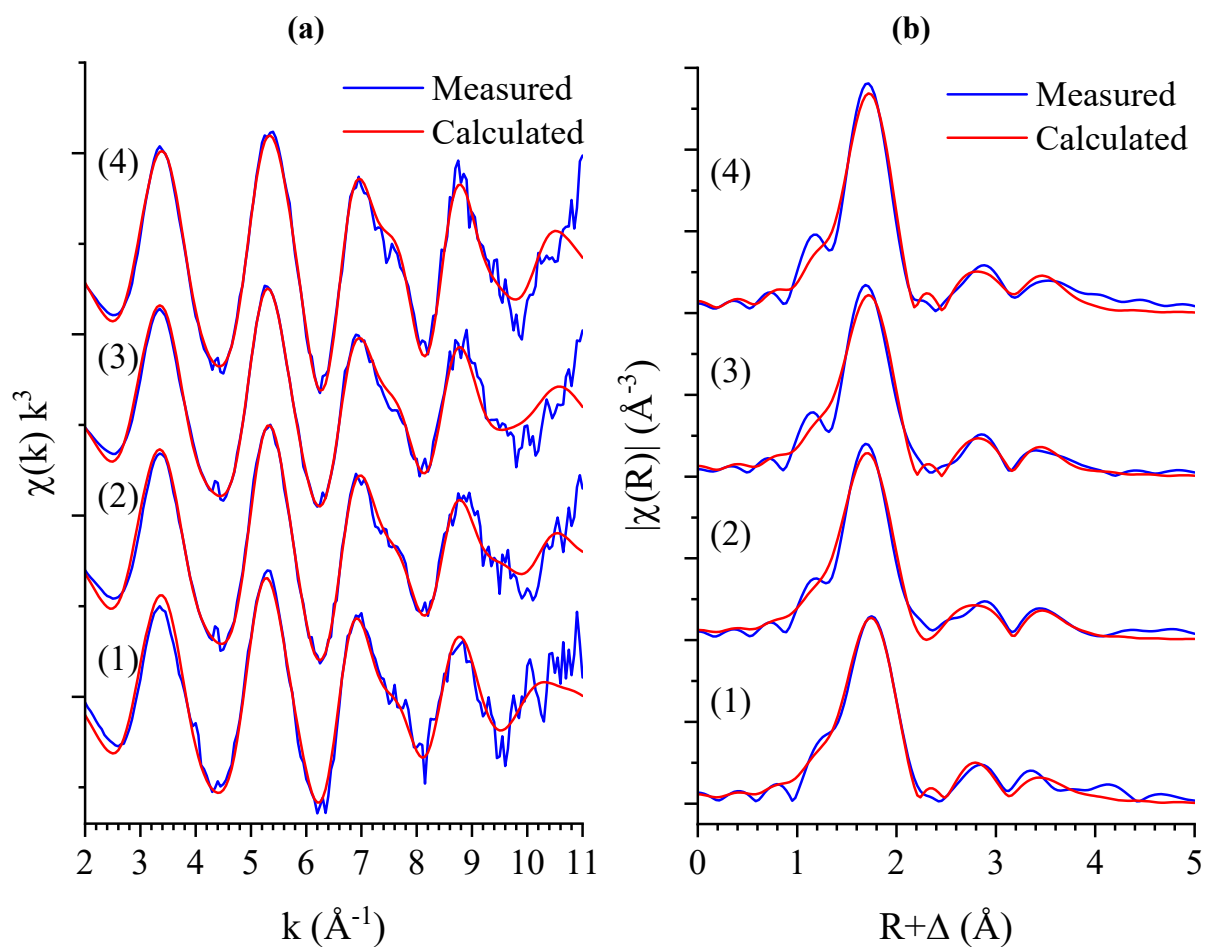


**Figure 6** EXAFS spectra  $2 \text{ \AA} < k < 11 \text{ \AA}$  (a) and respective Fourier Transform (b) at plutonium  $L_{III}$  edge for the Pu(IV)-silicate colloids solution for the reference sample (1), a sample filtered at  $0.45 \text{ \mu m}$  (2), a sample filtered at  $100 \text{ kDa}$  (3) and a sample filtered at  $100 \text{ kDa}$  1 year-old aged (4).

#### 4. CONCLUSION

Studying the speciation of Pu(IV) in very alkaline and silicate ions rich reactive media allowed identifying the formation of plutonium (IV)-silicate colloidal suspensions which were stable for months. Their structural characterization evidenced that their structure was very similar to those identified for the other actinide-silicate colloidal systems.<sup>2, 12-15</sup> These colloids were smaller than 6 nm in size, which was very close to that usually observed for PuO<sub>2</sub> nanoparticles,<sup>30, 32, 33</sup> probably leading to comparable properties in terms of mobility. The conditions tested allowed stabilizing colloidal suspensions for Pu(IV) concentration around 10<sup>-2</sup> mol·L<sup>-1</sup> and pH values up to 13 in silicate ions reactive media.

Based on these observations, the solubility increase observed for PuO<sub>2</sub> in alkaline silica solutions<sup>8, 11</sup> might be explained by the formation of such silicate colloids, which could affect the plutonium mobility. Specifically, it may partially explain the plutonium mobility in some contaminated sites, such as Mortandad Canyon,<sup>38, 39</sup> Savannah River,<sup>40</sup> the Nevada Test Site<sup>41</sup> or the Mayak production association.<sup>42</sup> Moreover, the formation of actinide bearing silicate colloids has to be considered in the field of high level radioactive waste storages, especially in permeable media. In this context, the identification of plutonium (IV)-silicate interactions constitutes the first step for a better understanding of plutonium environmental chemistry.

## ASSOCIATED CONTENT

### Supporting information

**Table S1** reporting the results of the UV-visible and pH monitoring of the solution resulting from the addition of Pu(IV) nitric solution in Na<sub>2</sub>SiO<sub>3</sub> 2 mol·L<sup>-1</sup> aqueous solution. **Table S2** gathering interatomic distances reported for ThSiO<sub>4</sub>, USiO<sub>4</sub>, CeSiO<sub>4</sub> and PuSiO<sub>4</sub>.<sup>26, 27, 43, 44</sup> **Table S3** reporting the structural parameters determined by EXAFS characterization for the actinide silicate colloids.<sup>2, 16-18</sup> **Figure S1** representing the pH monitoring of Na<sub>2</sub>SiO<sub>3</sub> 2 mol·L<sup>-1</sup> aqueous solution depending on the addition of Pu(IV) nitric solution. **Figure S2** representing the UV-visible spectra of a Pu(IV)-silicate solution freshly prepared and after a 3 months ageing. **Figure S3** reporting the picture of the Pu-silicate colloids solution filtrated at 0.1 μm and 3 kDa. This material is available free of charge via the Internet at <http://pubs.acs.org>.

## AUTHOR INFORMATION

### Corresponding author

\*N. D.: phone. +33 4 66 33 92 05; e-mail. [nicolas.dacheux@umontpellier.fr](mailto:nicolas.dacheux@umontpellier.fr)

\*T. D.: phone. + 33 4 66 79 65 87; e-mail. [thomas.dumas@cea.fr](mailto:thomas.dumas@cea.fr)

### ORCID

Paul Estevenon: [0000-0001-8517-4744](https://orcid.org/0000-0001-8517-4744)

Thomas Dumas: [0000-0001-6425-6484](https://orcid.org/0000-0001-6425-6484)

Éléonore Welcomme: [0000-0002-3758-6717](https://orcid.org/0000-0002-3758-6717)

Stéphanie Szenknect: [0000-0003-3691-3621](https://orcid.org/0000-0003-3691-3621)

Adel Mesbah: [0000-0002-6905-2402](https://orcid.org/0000-0002-6905-2402)

Kristina Kvashnina: [0000-0003-4447-4542](https://orcid.org/0000-0003-4447-4542)

Philippe Moisy: [0000-0002-9331-0846](https://orcid.org/0000-0002-9331-0846)

Christophe Poinssot: [0000-0002-6161-9582](https://orcid.org/0000-0002-6161-9582)

Nicolas Dacheux: [0000-0003-1636-1313](https://orcid.org/0000-0003-1636-1313)

### Notes

The authors declare no competing financial interest

## ACKNOWLEDGMENTS

The authors would like to thank V. Brethenoux and J. Hennuyer (from CEA) for supporting the syntheses experiments.

## REFERENCES

1. Gonzales, E.; Na, B. C.; Salvatores, M.; Zimmerman, C. H.; Varaine, F.; D'Angelo, A.; Schikorr, M.; Kuijper, J. C.; Coddington, P.; Kim, Y. H. *Physics and safety of transmutation systems - A status report*; Nuclear Energy Agency: 2006.
2. Hennig, C.; Weiss, S.; Banerjee, D.; Brendler, E.; Honkimäki, V.; Cuello, G.; Ikeda-Ohno, A.; Scheinost, A. C.; Zänker, H. Solid-state properties and colloidal stability of thorium(IV)-silica nanoparticles. *Geochimica et Cosmochimica Acta* **2013**, 103, 197-212.
3. Dreissig, I.; Weiss, S.; Hennig, C.; Bernhard, G.; Zänker, H. Formation of uranium(IV)-silica colloids at near-neutral pH. *Geochimica et Cosmochimica Acta* **2011**, 75, 352-367.
4. Husar, R.; Weiss, S.; Hennig, C.; Hübner, R.; Ikeda-ohno, A.; Zänker, H. Formation of Neptunium(IV) – Silica Colloids at Near-Neutral and Slightly Alkaline pH. *Environmental Science & Technology* **2015**, 49, 665-671.
5. Yusov, A. B.; Fedoseev, A. M.; Delegard, C. H. Hydrolysis of Np(IV) and Pu(IV) and their complexation by aqueous Si(OH)<sub>4</sub>. *Radiochimica Acta* **2004**, 92, 869-881.
6. Pazukhin, E. M.; Krivokhatskii, A. S.; Kudryatsev, E. G. Possible formation of Pu(IV) complexes with silicic acid. *Soviet Radiochemistry* **1990**, 32, 26-32.
7. Neck, V.; Kim, J. I. Solubility and hydrolysis of tetravalent actinides. *Radiochimica Acta* **2001**, 89, 1-16.
8. Shilov, V. P.; Fedoseev, A. M. Solubility of Pu(IV) in Weakly Alkaline Solutions (pH 9-14) Containing Silicate Anions. *Radiokhimiya* **2003**, 45, 491-494.
9. Erickson, H. P. Size and shape of protein molecules at the nanometer level determined by sedimentation, gel filtration, and electron microscopy. *Biological Procedures Online* **2009**, 15, 32-51.
10. Jensen, M. P. Competitive complexation studies of europium(III) and uranium(VI) complexation by aqueous orthosilicic acid. Ph.D. Thesis. Florida State University, Tallahassee, FL, United States, 1994.
11. Rai, D.; Yui, M.; Moore, D. A.; Lumetta, G. J.; Rosso, K. M.; Xia, Y.; Felmy, A. R.; Skomurski, F. N. Thermodynamic model for ThO<sub>2</sub>(am) solubility in alkaline silica solutions. *Journal of Solution Chemistry* **2008**, 37, 1725-1746.
12. Riglet-Martial, C.; Laszak, I.; Bion, L.; Vitorge, P. *Competition carbonate-silicate sur la complexation des actinides en milieu argileux riche en silice*; CEA: 2000.
13. Peretroukhine, V.; Riglet-Martial, C.; Capdevila, H.; Calmon, V.; Bienvenu, P.; Laszak, I. Effect of soluble silicates on the solubility of thorium(IV) hydrous oxide. *Journal of Nuclear Science and Technology* **2002**, Supplement, 516-519.
14. Zänker, H.; Hennig, C. Colloid-borne forms of tetravalent actinides : A brief review. *Journal of Contaminant Hydrology* **2014**, 157, 87-105.
15. Zänker, H.; Weiss, S.; Hennig, C.; Brendler, V.; Ikeda-Ohno, A. Oxyhydroxy silicate colloids: a new type of waterborne actinide(IV) colloids. *Chemistry Open* **2016**, 5, 174-182.
16. Ulbricht, I. Bildung von Kolloiden des tetravalenten Urans unter Einfluss von Silikat in neutralen und schwachalkalischen wässrigen Systemen. Ph.D. Thesis. Technischen Universität Dresden, Dresden, Germany, 2010.
17. Neill, T. S.; Morris, K.; Pearce, C. I.; Sherriff, N. K.; Burke, M. G.; Chater, P. A.; Janssen, A.; Natrajan, L. S.; Shaw, S. Stability, composition and core-shell particle structure of uranium(IV)-silicate colloids. *Environmental Science & Technology* **2018**, 52, 9118–9127.
18. Husar, R. Investigation into the formation of nanoparticles of tetravalent neptunium in slightly alkaline aqueous solution. Ph.D. Thesis. Technischen Universität Dresden, Dresden, Germany, 2015.
19. Stumm, W.; Hüper, H.; Champlin, L. Formation of polysilicates as determined by coagulation effects. *Environmental Science and Technology* **1967**, 1, 221-227.

20. Speer, J. A. The actinide orthosilicates. *Reviews in Mineralogy and Geochemistry* **1980**, 5, 113-135.
21. Kaya, A.; Kud, H.; Shirahashi, J.; Suzuki, S. The purification of plutonium by anion exchange in nitric acid. *Journal of Nuclear Science and Technology* **1967**, 4, 289-292.
22. Livshits, M. A.; Khomyakova, E.; Evtushenko, E. G.; Lazarev, V. N.; Kulemin, N. A.; Semina, S. E.; Generozov, E. V.; Govorun, V. M. Isolation of exosomes by differential centrifugation: theoretical analysis of a commonly used protocol. *Scientific Reports* **2015**, 5, 17319.
23. Llorens, I.; Solari, P. L.; Sitaud, B.; Bes, R.; Cammelli, S.; Hermange, H.; Othmane, G.; Safi, S.; Moisy, P.; Wahu, S.; Bresson, C.; Schlegel, M. L.; Menut, D.; Bechade, J. L.; Martin, P.; Hazemann, J. L.; Proux, O.; Den Auwer, C. X-ray absorption spectroscopy investigations on radioactive matter using MARS beamline at SOLEIL synchrotron. *Radiochimica Acta* **2014**, 102, 957-972.
24. Ravel, B.; Newville, M. ATHENA, ARTEMIS, HEPHAESTUS: data analysis for X-ray absorption spectroscopy using IFEFFIT. *Journal of Synchrotron Radiation* **2005**, 12, 537-541.
25. Ankudinov, A. L.; Ravel, B.; Rehr, J. J.; Conradson, S. D. Realspace multiple-scattering calculation and interpretation of x-ray absorption near-edge structure. *Physica B: Condensed Matter* **1998**, 58, 7565-7576.
26. Keller, C. Untersuchungen über die Germanate und Silikate des Typs  $ABO_4$  der vierwertigen Elemente Thorium bis Americium. *Nukleonik* **1963**, 5, 41-48.
27. Skakle, J. M. S.; Dickson, C. L.; Glasser, F. P. The crystal structures of  $CeSiO_4$  and  $Ca_2Ce_8(SiO_4)_6O_2$ . *Powder diffraction* **2000**, 15, 234-238.
28. Paul, A. *Chemistry of Glasses*. Springer Netherlands: 1982.
29. Giffaut, E.; Grivé, M.; Blanc, P.; Vieillard, P.; Colàs, E.; Gailhanou, H.; Gaboreau, S.; Marty, N.; Madé, B.; Duro, L. Andra thermodynamic database for performance assessment: ThermoChimie. *Applied Geochemistry* **2014** 49, 225-236.
30. Dalodière, E.; Viro, M.; Morosini, V.; Chave, T.; Dumas, T.; Hennig, C.; Wiss, T.; Dieste Blanco, O.; Shuh, D. K.; Tyliszczak, T.; Venault, L.; Nikitenko, S. I. Insights into the sonochemical synthesis and properties of salt-free intrinsic plutonium colloids. *Scientific Reports* **2017**, 7, 43514.
31. Hudry, D.; Apostolidis, C.; Walter, O.; Janßen, A.; Manara, D.; Griveau, J.-C.; Colineau, E.; Vitova, T.; Prößmann, T.; Wang, D.; Kübel, C.; Meyer, D. Ultra-small plutonium oxide nanocrystals: an innovative material in plutonium science. *Chemistry - A European Journal* **2014**, 20, 10431-10438.
32. Bonato, L.; Viro, M.; Dumas, T.; Mesbah, A.; Dalodière, E.; Dieste Blanco, O.; Wiss, T.; Le Goff, X.; Odorico, M.; Prieur, D.; Rossberg, A.; Venault, L.; Dacheux, N.; Moisy, P.; Nikitenko, S. I. Probing the local structure of nanoscale actinide oxides: a comparison between  $PuO_2$  and  $ThO_2$  nanoparticles rules out  $PuO_{2+x}$  hypothesis. *Nanoscale Advances* **2020**, 2, 214-224.
33. Gerber, E.; Romanchuk, A. Y.; Pidchenko, I.; Amidani, L.; Rossberg, A.; Hennig, C.; Vaughan, G. B. M.; Trigub, A.; Egorova, T.; Bauters, S.; Plakhova, T.; Hunault, M. O. J. Y.; Weiss, S.; Butorin, S. M.; Scheinost, A. C.; Kalmykov, S. N.; Kvashnina, K. O. The missing pieces of the  $PuO_2$  nanoparticle puzzle. *Nanoscale* **2020**, 12, 18039-18048.
34. Micheau, C.; Viro, M.; Dourdain, S.; Dumas, T.; Menut, D.; Solari, P. L.; Venault, L.; Diat, O.; Moisy, P.; Nikitenko, S. I. Relevance of formation conditions to the size, morphology and local structure of intrinsic plutonium colloids. *Environmental Science: Nano* **2020**, 7, 2252-2266.

35. Rothe, J.; Walther, C.; Denecke, M. A.; Fanghänel, T. XAFS and LIBD Investigation of the Formation and Structure of Colloidal Pu(IV) Hydrolysis Products. *Inorganic Chemistry* **2004**, *43*, 4708-4718.
36. Ekberg, C. L., K.; Skarnemark, G. Ö.-J., A.; Persson, I. The structure of plutonium(IV) oxide as hydrolysed clusters in aqueous suspensions *Dalton Transactions* **2013**, *42*, 2035-2040
37. Shannon, R. D. Revised effective ionic radii and systematic studies of interatomic distances in halides and chalcogenides. *Acta Crystallographica Section A*. **1976**, *32*, 751-767.
38. Penrose, W. R.; Polzer, W. L.; Essington, E. H.; Nelson, D. M.; Orlandini, K. A. Mobility of plutonium and americium through a shallow aquifer in a semiarid region. *Environmental Science & Technology* **1990**, *24*, 228-234.
39. Marty, R. C.; Bennett, D.; Thullen, P. Mechanism of plutonium transport in a shallow aquifer in Mortandad Canyon, Los Alamos National Laboratory, New Mexico. *Environmental Science & Technology* **1997**, *31*, 2020-2027.
40. Kaplan, D. I.; Bertsch, P. M.; Adriano, D. C.; Orlandini, K. A. Actinide association with groundwater colloids in a coastal plain aquifer. *Radiochimica Acta* **1994**, *66-67*, 181-187.
41. Kersting, A. B.; Efurud, D. W.; Finnegan, D. L.; Rokop, D. J.; Smith, D. K.; Thompson, J. L. Migration of plutonium in ground water at the Nevada Test Site. *Nature* **1999**, *397*, 56-59.
42. Novikov, A. P.; Kalmykov, S. N.; Utsunomiya, S.; Ewing, R. C.; Horreard, F.; Merkulov, A.; Clark, S. B.; Tkachev, V. V.; Myasoedov, B. F. Colloid transport of plutonium in the far-field of the Mayak production association, Russia. *Science* **2006**, *314*, 638-641.
43. Taylor, M.; Ewing, R. C. The crystal structures of the ThSiO<sub>4</sub> polymorphs: huttonite and thorite. *Acta Crystallographica Section B-Structural Crystallography and Crystal Chemistry* **1978**, *34*, 1074-1079.
44. Fuchs, L. H.; Gebert, E. X-ray studies of synthetic coffinite, thorite and uranothorites. *The American Mineralogist* **1958**, *43*, 243-248.

# Formation of plutonium (IV) silicate species in very alkaline reactive media

Paul Estevenon<sup>1,2,3,4</sup>, Thomas Dumas<sup>1,\*</sup>, Pier Lorenzo Solari<sup>5</sup>, Eleonore Welcomme<sup>1</sup>,  
Stephanie Szenknect<sup>2</sup>, Adel Mesbah<sup>2</sup>, Kristina O. Kvashnina<sup>3,4</sup>, Philippe Moisy<sup>1</sup>, Christophe  
Poinssot<sup>1</sup>, Nicolas Dacheux<sup>2,\*</sup>

<sup>1</sup> CEA, DES, ISEC, DMRC, Univ Montpellier, Marcoule, France.

<sup>2</sup> ICSM, Univ Montpellier, CNRS, CEA, ENSCM, Bagnols-sur-Cèze, France

<sup>3</sup> The Rossendorf Beamline at the European Synchrotron, CS40220, 38040 Grenoble Cedex 9, France.

<sup>4</sup> Helmholtz Zentrum Dresden-Rossendorf (HZDR), Institute of Resource Ecology, P.O. Box 510119, 01314, Dresden, Germany.

<sup>5</sup> Synchrotron SOLEIL L'Orme des Merisiers, Saint-Aubin, BP 48, F-91192 Gif-sur-Yvette Cedex France

## SUPPORTING INFORMATION

**Table S1** Results of the pH and UV-visible monitoring on a  $\text{Na}_2\text{SiO}_3$   $2 \text{ mol}\cdot\text{L}^{-1}$  aqueous solution depending on the addition of Pu(IV) nitric solution ( $C_{\text{HNO}_3} = 1.5 \text{ mol}\cdot\text{L}^{-1}$ ;  $C_{\text{Pu}} = 0.3 \text{ mol}\cdot\text{L}^{-1}$ ).

V( $\text{Na}_2\text{SiO}_3$ 2M)	V(Pu 0.3M in $\text{HNO}_3$ 1.5M)	pH	UV-visible spectroscopy observations
0.800 mL	0 mL	13.3	-
	0.100 mL	13.3	Pu(IV)-silicate species
	0.100 mL	13.2	Pu(IV)-silicate species
	0.100 mL	13.1	Pu(IV)-silicate species
	0.400 mL	13.0	Pu(IV)-silicate species
	0.500 mL	12.5	Pu(IV)-silicate species (weak intensity)
	0.600 mL	12.0	No Pu species observed
	0.700 mL	11.4	No Pu species observed
	0.900 mL	9.6	No Pu species observed
	1.000 mL	2.5	No Pu species observed

**Table S2** Interatomic distances for  $\text{ThSiO}_4$ ,  $\text{USiO}_4$ ,  $\text{CeSiO}_4$  and  $\text{PuSiO}_4$  (zircon type silicates, space group  $I4_1/amd$ <sup>20</sup>).

	Interatomic distances ( $\text{ASiO}_4$ )				Abundance
	$\text{ThSiO}_4$ <sup>43</sup>	$\text{USiO}_4$ <sup>44</sup>	$\text{CeSiO}_4$ <sup>27</sup>	$\text{PuSiO}_4$ <sup>26</sup>	
A-O <sub>1</sub>	2.46 Å	2.32 Å	2.27 Å	-	4
A-O <sub>2</sub>	2.56 Å	2.51 Å	2.37 Å	-	4
A-Si <sub>1</sub> (bidentate)	3.16 Å	3.13 Å	3.10 Å	3.11 Å	2
A-Si <sub>2</sub> (monodentate)	3.91 Å	3.83 Å	3.81 Å	3.79 Å	4
A-A	3.91 Å	3.83 Å	3.81 Å	3.79 Å	4

**Table S3** Structural parameters for the Pu(IV)-silicate species determined in this study and reported in the literature for Th(IV)-, U(IV)- and Np(IV)-silicates colloids. The values fixed for the simulations have been marked by an asterisk.

<b>Plutonium (IV)-silicate species (this study)</b>					
Reference	R (Å)	N	$\sigma^2$ (Å <sup>2</sup> )	$\Delta E_{k=0}$	F
Pu-O <sub>1</sub>	2.23 (2) Å	4 *	0.007 (3)	- 1.2 eV	0.02
Pu-O <sub>2</sub>	2.34 (3) Å	4 *	0.007 (3)		
Pu-Si <sub>1</sub>	3.21 (6) Å	1.1 (9)	0.009*		
Pu-Si <sub>2</sub>	3.46 (3) Å	5.4 (22)	0.012*		
Pu-Pu	3.77 (3) Å	6.0 (21)	0.020 (26)		
Filtered 0.45 $\mu$ m					
Pu-O <sub>1</sub>	2.20 (1) Å	4 *	0.005 (2)	- 2.8 eV	0.03
Pu-O <sub>2</sub>	2.33 (2) Å	4 *	0.005 (2)		
Pu-Si <sub>1</sub>	3.04 (7) Å	2.1 (6)	0.009*		
Pu-Si <sub>2</sub>	3.49 (3) Å	5.3 (19)	0.012*		
Pu-Pu	3.73 (3) Å	5.1 (39)	0.017 (8)		
Filtered 100 kDa					
Pu-O <sub>1</sub>	2.24 (37) Å	4 *	0.007 (3)	- 2.7 eV	0.02
Pu-O <sub>2</sub>	2.30 (38) Å	4 *	0.007 (3)		
Pu-Si <sub>1</sub>	3.26 (14) Å	0.7 (18)	0.009*		
Pu-Si <sub>2</sub>	3.47 (5) Å	6.1 (39)	0.012*		
Pu-Pu	3.73 (4) Å	6.4 (32)	0.020 (1)		
1 year-old					
Pu-O <sub>1</sub>	2.23 (17) Å	4 *	0.007 (3)	- 2.3 eV	0.04
Pu-O <sub>2</sub>	2.29 (18) Å	4 *	0.007 (3)		
Pu-Si <sub>1</sub>	3.26 (8) Å	1.1 (6)	0.009*		
Pu-Si <sub>2</sub>	3.46 (3) Å	8.8 (19)	0.012*		
Pu-Pu	3.75 (3) Å	3.9 (39)	0.013 (7)		
<b>Thorium (IV)-silicate colloids <sup>2</sup></b>					
Th/Si = 1.4	R (Å)	N	$\sigma^2$ (Å <sup>2</sup> )	$\Delta E_{k=0}$	F
Th-O	2.39 Å	8.9	0.016	- 0.9 eV	0.10
Th-Si	3.26 Å	1.3	0.011		
Th/Si = 1.7					
Th-O	2.38 Å	8.6	0.016	- 1.6 eV	0.07
Th-Si	3.25 Å	1.6	0.013		
Th/Si = 5.8					
Th-O	2.36 Å	8.3	0.018	- 2.1 eV	0.09
Th-Si	3.23 Å	2.5	0.011		
<b>Uranium (IV)-silicate colloids <sup>16</sup></b>					
Si/U = 0.83	R (Å)	N	$\sigma^2$ (Å <sup>2</sup> )	$\Delta E_{k=0}$	F
U-O <sub>1</sub>	2.25 Å	4.1	0.0082	- 19 eV	0.19
U-O <sub>2</sub> /Si	2.81 Å	2.7	0.0082		
U-U	3.85 Å	2.6	0.0067	- 6 eV	
Si/U = 1.68					
U-O <sub>1</sub>	2.23 Å	2.7	0.0081	- 16 eV	0.16
U-O <sub>2</sub> /Si	2.83 Å	3.5	0.0081		

<b>Uranium (IV)-silicate colloids <sup>17</sup></b>					
4 mM <sub>Si</sub> pH = 9	R (Å)	N	$\sigma^2$ (Å <sup>2</sup> )	$\Delta E_{k=0}$	F
U-O <sub>1</sub>	2.26 (1) Å	4.3	0.009 (1)	4.1 (10) eV	0.0124
U-O <sub>2</sub>	2.44 (1) Å	3.8	0.009 (1)		
U-Si <sub>1</sub>	3.17 (2) Å	1.1	0.010 (3)		
U-Si <sub>2</sub>	3.70 (3) Å	2.5	0.013 (4)		
U-U	3.78(5) Å	1	0.013(7)		
<b>4 mM<sub>Si</sub> pH = 10.5</b>					
U-O <sub>1</sub>	2.28 (1) Å	4.5	0.006 (1)	5.5 (9) eV	0.0076
U-O <sub>2</sub>	2.46 (1) Å	3.5	0.006 (1)		
U-Si <sub>1</sub>	3.18 (2) Å	1.6	0.011 (3)		
U-Si <sub>2</sub>	3.73 (4) Å	2	0.014 (5)		
U-U	3.79 (4) Å	1.8	0.014 (5)		
<b>4 mM<sub>Si</sub> pH = 12</b>					
U-O <sub>1</sub>	2.29 (1) Å	4.4	0.007 (1)	6.1 (6) eV	0.0042
U-O <sub>2</sub>	2.46 (1) Å	3.0	0.007 (1)		
U-Si <sub>1</sub>	3.19 (2) Å	1.6	0.013 (3)		
U-Si <sub>2</sub>	3.71 (5) Å	0.8	0.012 (7)		
U-U	3.84 (2) Å	2.8	0.013 (2)		
<b>2 mM<sub>Si</sub> pH = 9</b>					
U-O <sub>1</sub>	2.28 (1) Å	3.7	0.008 (1)	6.5 (5) eV	0.0024
U-O <sub>2</sub>	2.47 (1) Å	3.9	0.008 (1)		
U-Si <sub>1</sub>	3.19 (1) Å	1	0.009 (2)		
U-Si <sub>2</sub>	3.76 (3) Å	1	0.013 (2)		
U-U	3.85 (1) Å	2.5	0.013 (4)		
<b>2 mM<sub>Si</sub> pH = 10.5</b>					
U-O <sub>1</sub>	2.28 (1) Å	4.4	0.007 (1)	4.5 (8) eV	0.0124
U-O <sub>2</sub>	2.45 (1) Å	3.5	0.007 (1)		
U-Si <sub>1</sub>	3.17 (2) Å	0.9	0.007 (3)		
U-Si <sub>2</sub>	3.74 (4) Å	1.5	0.011 (5)		
U-U	3.80 (3) Å	2.6	0.013 (3)		
<b>2 mM<sub>Si</sub> pH = 12</b>					
U-O <sub>1</sub>	2.30 (1) Å	4.7	0.005 (1)	6.2 (8) eV	0.0121
U-O <sub>2</sub>	2.46 (1) Å	3.3	0.005 (1)		
U-Si <sub>1</sub>	3.18 (3) Å	1	0.009 (5)		
U-Si <sub>2</sub>	3.75 (5) Å	1.8	0.014 (7)		
U-U	3.86 (2) Å	5	0.015 (2)		
<b>Neptunium (IV)-silicate colloids <sup>18</sup></b>					
	R (Å)	N	$\sigma^2$ (Å <sup>2</sup> )	$\Delta E_{k=0}$	F
Np-O	2.28(1) Å	7.1(2)	0.017(4)	-9.3 eV	0.07
Np-Si	3.11(1) Å	1.3(1)	0.0091(2)		
Np-Np	3.75(2) Å	1.1(1)	0.0098(1)		

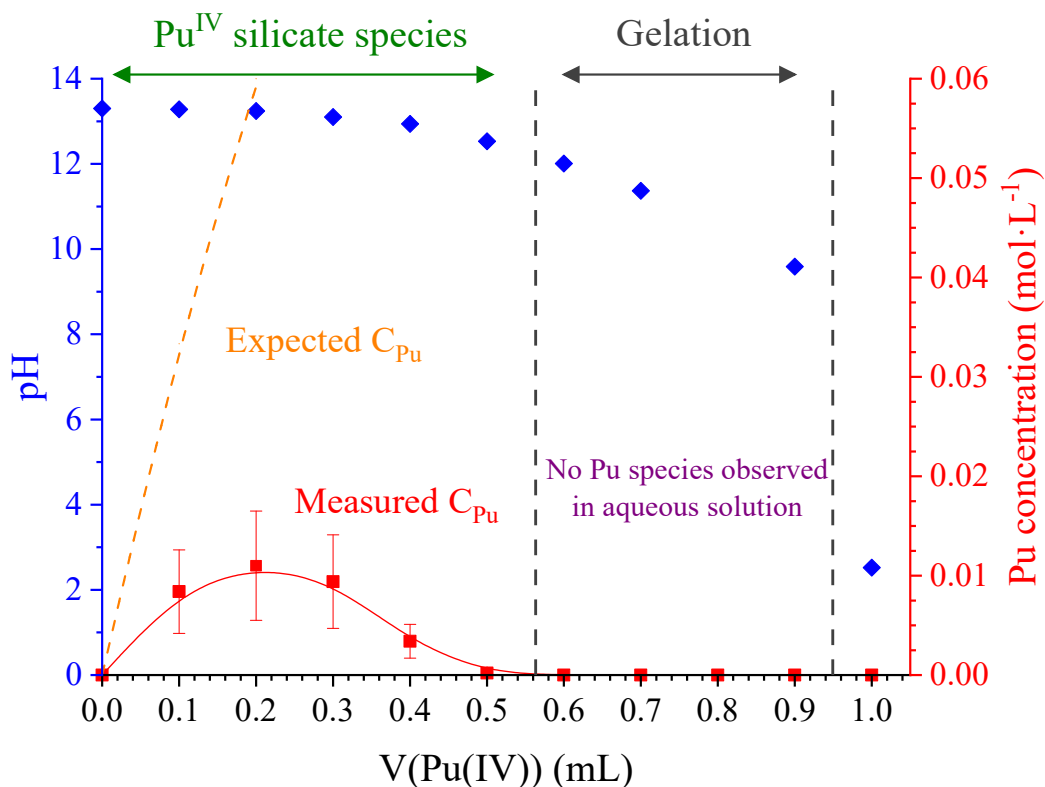


**Figure S1** pH monitoring of a  $2 \text{ mol}\cdot\text{L}^{-1}$  aqueous  $\text{Na}_2\text{SiO}_3$  solution depending on the addition of Pu(IV) nitric solution ( $C_{\text{HNO}_3} = 1.5 \text{ mol}\cdot\text{L}^{-1}$  ;  $C_{\text{Pu}} = 0.3 \text{ mol}\cdot\text{L}^{-1}$ ), according to **Table S1**. The measured plutonium concentration was determined from the UV-visible spectra by Beer-Lambert law and the expected concentration is corresponding to the plutonium amount added to the system.

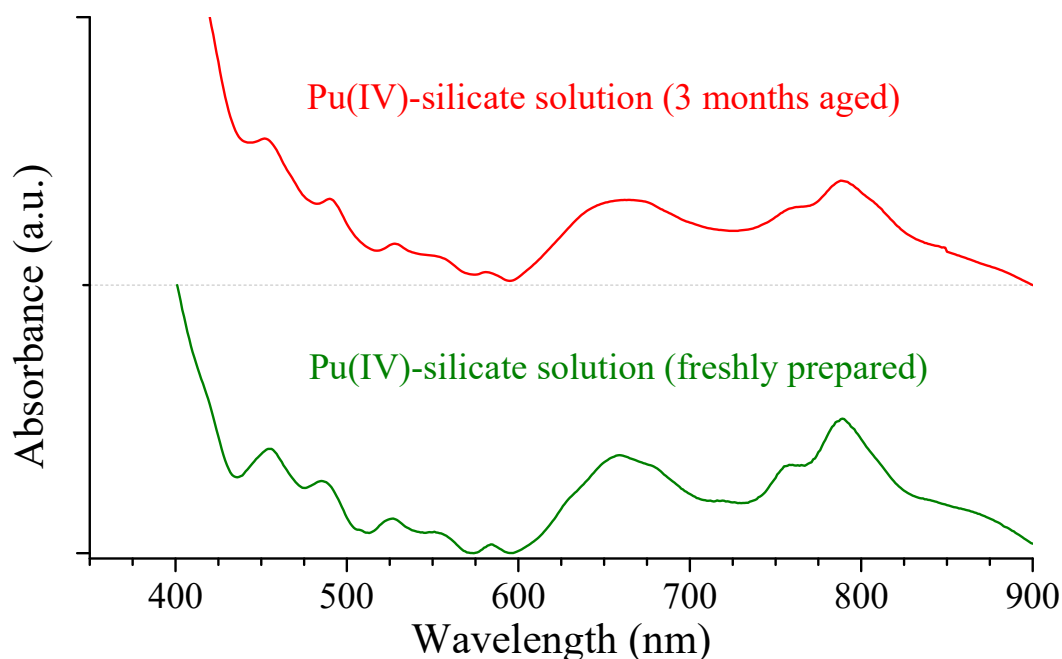


**Figure S2** UV-visible spectra of a Pu(IV)-silicate solution ( $\text{pH} = 13.2$ ,  $C_{\text{Na}_2\text{SiO}_3} \approx 2 \text{ mol}\cdot\text{L}^{-1}$ ,  $C_{\text{Pu}} = 3 \times 10^{-2} \text{ mol}\cdot\text{L}^{-1}$ ) freshly prepared and after a 3 months ageing.

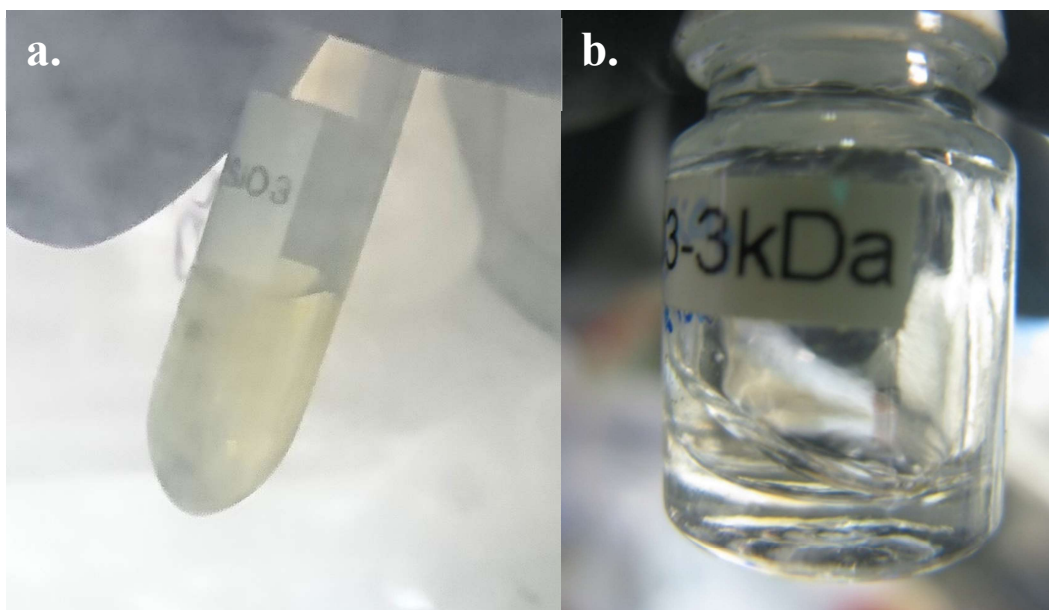


**Figure S3** Pu(IV)-silicate solution ( $\text{pH} = 13.2$ ,  $C_{\text{Na}_2\text{SiO}_3} \approx 2 \text{ mol}\cdot\text{L}^{-1}$ ) filtrated at  $0.1 \mu\text{m}$  (a.) and  $3 \text{ kDa}$  (b.).

(a)

(b)

**Figure S4** EXAFS spectra  $2 \text{ \AA} < k < 11 \text{ \AA}$  (a) and respective Fourier Transform (b) at plutonium  $L_{\text{III}}$  edge for a Pu(IV)-silicate solution filtered at  $0.45 \mu\text{m}$ .

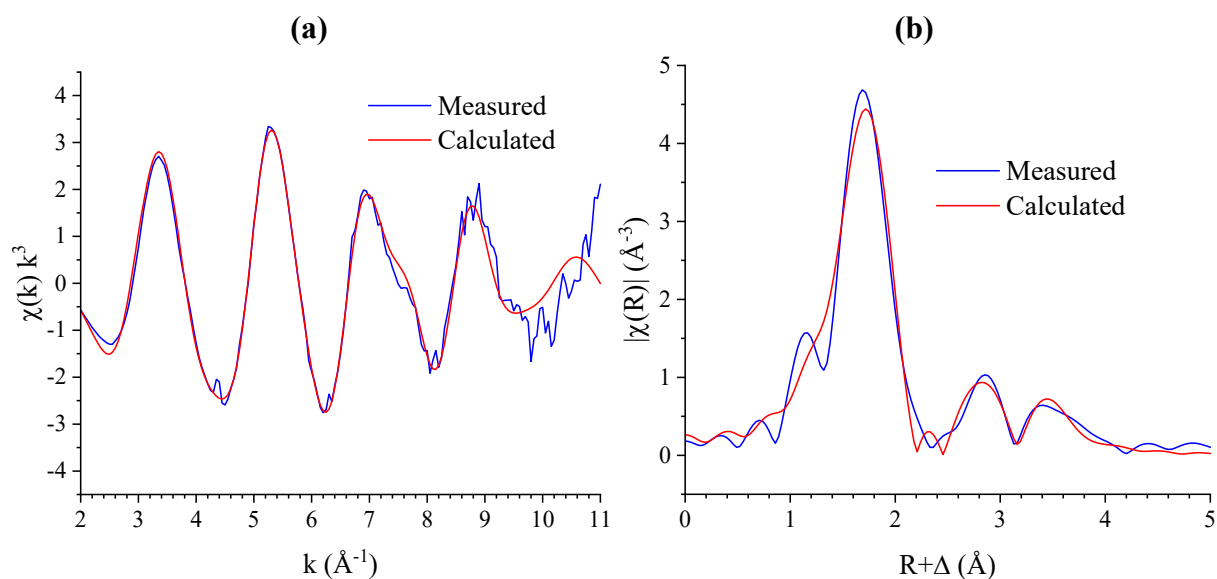


**Figure S5** EXAFS spectra  $2 \text{ \AA} < k < 11 \text{ \AA}$  (a) and respective Fourier Transform (b) at plutonium  $L_{III}$  edge for a Pu(IV)-silicate solution filtered at 100 kDa.

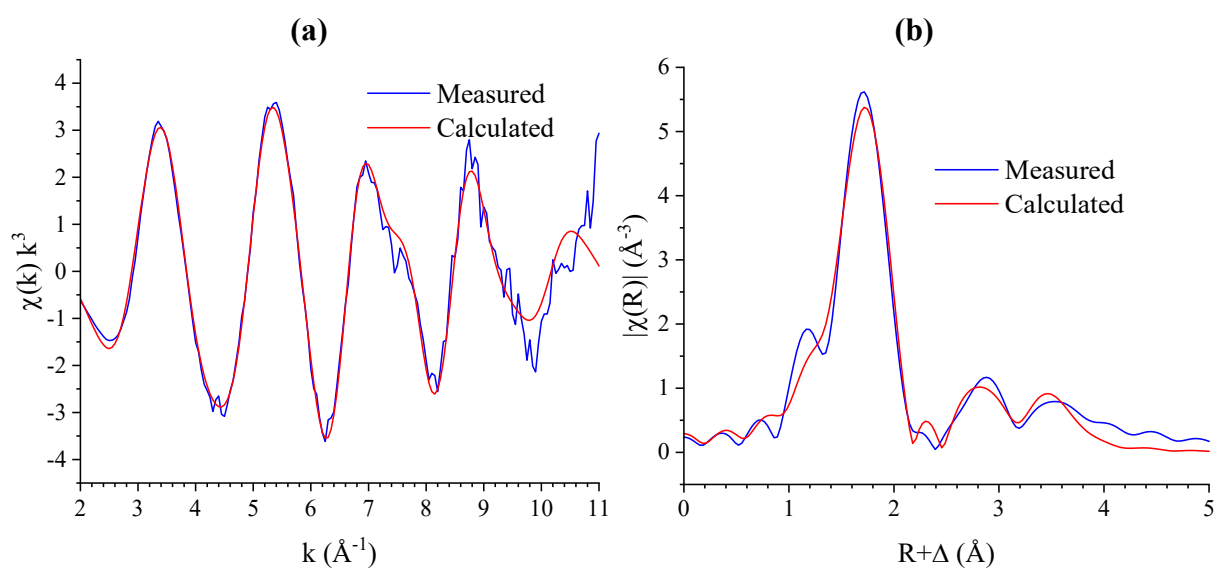


**Figure S6** EXAFS spectra  $2 \text{ \AA} < k < 11 \text{ \AA}$  (a) and respective Fourier Transform (b) at plutonium  $L_{III}$  edge for a Pu(IV)-silicate solution filtered at 100 kDa and 1 year old aged.

## FOR TABLE OF CONTENTS ONLY

This article highlights how Pu(IV) solubility is highly impacted by the presence of silicate ions in very alkaline reactive media. Thanks to XAS characterization, sequential filtration process and alpha spectrometry, the formation of Pu(IV)-silicate colloids with a particle size below 6 nm at a 10 mM concentration has been evidenced. As reported in the literature for the other actinide silicate systems, the formation of these species may dramatically impact the plutonium mobility in the environment.

